Wide-bandwidth 25-dB amplitude noise suppression in a pump-and-signal-resonant optical parametric oscillator

M. J. Lawrence and R. L. Byer

Ginzton Laboratory, Stanford University, Stanford, California 94305

M. A. Arbore and J. D. Kmetec

Lightwave Electronics Corporation, 2400 Charleston Road, Mountain View, California 94043

Received February 7, 2001

We present a pump-and-signal-resonant optical parametric oscillator that provides 25 dB of amplitude noise suppression of the transmitted pump beam from dc to 20 kHz. The upper frequency range of the optical limiter increases as the pump power is increased, up to 1 MHz with 580 mW of input power. The amount of noise suppression is limited by pump-depletion effects. The upper frequency range is limited by the temporal response of the device. We present a numerical analysis that predicts this behavior. © 2001 Optical Society of America

OCIS codes: 190.4970, 230.4320, 140.3070.

Ultralow-noise lasers are required for the Laser Interferometer Gravitational-Wave Observatory. Current approaches to developing such lasers (electronic feedback and passive cavities) are limited in frequency and dynamic range. Siegman suggested the use of an optical parametric oscillator (OPO) as an optical power limiter in 1962,[1] three years before the first OPO was constructed.[2] After the first OPO demonstration, initially rapid progress was limited by the immaturity of laser sources and nonlinear materials. The development of stable diode-pumped solid-state lasers[3] led to the first cw singly resonant OPO in 1993.[4] Subsequently, higher nonlinear coefficients provided by periodically poled materials helped reduce the threshold power[5] of the stable singly resonant OPO configuration. Further reduction in threshold is possible if the pump is resonant along with the signal. The efficiency of such a device has been thoroughly studied.[6] However, an analytical approach does not simply account for the limitations on noise suppression that are due to pump depletion, and to our knowledge the noise-suppression properties of OPOs have not been quantified to date.

The bow-tie OPO used in this experiment[7] was resonant at both the pump and the signal frequencies. Above threshold, increasing input power initially results in higher gain for the signal field. The signal responds by growing at the expense of the circulating pump power until signal gain is equal to signal loss and a steady state is achieved. Since the round-trip signal losses remain constant and the signal gain is determined primarily by the circulating pump power, the circulating pump power is thus kept at a constant level. Fluctuations in the input field are not present in the circulating pump field, and noise suppression occurs. This interaction in a pump-resonant OPO configuration was first identified in 1966,[8] and clamping of the pump field, first seen in a long-pulse doubly resonant OPO,[9] has been observed in several OPO configurations.

As a result of depletion (i.e., gain saturation) effects, neither clamping nor noise suppression is perfect. Spatially, the signal field grows as it travels through the nonlinear medium. The pump field correspondingly decreases, resulting in an axial dependence in the pump field amplitude along the crystal. If the pump field amplitude at the end of the crystal decreases because of gain saturation, its value at the input must increase to provide the same single-pass (net) gain for the signal field. This increase of the circulating pump field at the input of the crystal and decrease at the exit results in imperfect clamping and imperfect noise suppression.

Theoretical analysis of the steady-state behavior of the pump-and-signal-resonant OPO configuration is possible by numerical solution of the steady-state plane-wave coupled nonlinear interaction equations.[10] Cavity resonances are accounted for by boundary conditions. That is, the initial pump and signal fields are the previous values calculated at the end of the crystal reflected around the cavity and, in the case of the pump, added to the coupled input pump. This self-consistent approach accurately reflects impedance matching of the input pump field. One can model the noise behavior by adding a small term δE_{in} to the input field. Propagation of this term through the time-dependent coupled nonlinear equations results in

$$\begin{aligned} \mathrm{d}\delta E_p/\mathrm{d}z &= -\alpha_p \delta E_p - i\kappa_p (E_s \delta E_i + \delta E_s E_i), \\ \mathrm{d}\delta E_s/\mathrm{d}z &= -\alpha_s \delta E_s - i\kappa_s (E_i^{*} \delta E_p + \delta E_i^{*} E_p), \\ \mathrm{d}\delta E_i/\mathrm{d}z &= -\alpha_i \delta E_i - i\kappa_i (E_s^{*} \delta E_p + \delta E_s^{*} E_p), \end{aligned} \quad (1)$$

where the subscripts p, s, and i stand for pump, signal, and idler, respectively; E is the envelope of the electromagnetic field; z is the distance along the nonlinear medium; α is loss within the medium; and κ is the nonlinear coupling term, given by $\omega h d_{\text{eff}}/nc$, where

0146-9592/01/141087-03$15.00/0

ω is the optical frequency, h is the Boyd–Kleinman focusing parameter,[11] d_{eff} is the effective nonlinear coefficient, n is the index of refraction, and c is the speed of light. The same boundary conditions are applied to the noise terms as for the steady-state terms.

In our experiment the nonlinear material was a 1-mm-thick, 2-cm-long crystal of periodically poled lithium niobate kept at 230 °C in a temperature-controlled oven.[12] The crystal was nominally antireflection coated, with 0.1% reflection at the pump and signal wavelengths and ≈10% at the idler wavelength. For the pump wavelength of 1064 nm the cavity consisted of a 5% power input coupler and three highly reflective mirrors. For the signal wavelength of 1547 nm the cavity consisted of a 3% power output coupler and three highly reflective mirrors. The generated idler at 3408 nm was removed from the cavity primarily by a mirror that was highly transmissive at this wavelength.

Resonance at the pump wavelength was maintained by rf locking,[13] with feedback to the fine-frequency input of our Lightwave Electronics Model 126 laser. The pump output was transmitted through a highly reflective (≈99.9%) mirror between the input coupler and the crystal. Noise measurements were performed with a reverse-biased ETX 1000T photodiode and a CLC436 operational amplifier in a transimpedance configuration.

Measured and theoretical steady-state behavior of this OPO is shown in Fig. 1. We fitted theory to experimental data by fitting the pump loss at the crystal faces to the below-threshold behavior. Above threshold, the signal loss at the crystal faces and the corrected effective nonlinear coefficient, hd_{eff}, were the fitted parameters. The resulting pump loss was 1.1%, and the signal loss was slightly higher at 1.4%. Larger loss is expected for the larger wavelength, which supports a larger mode, subject to more clipping at the crystal face edges. The fitted value for hd_{eff}, where h accounts for the decrease in coupling relative to an idealized plane-wave interaction that is due to diffraction and the Gaussian intensity profiles of the beams,[11] was 6.5 pm/V. This fitted value is close to the theoretical value of 4.6 pm/V, given by a predicted value[14] of 0.27 for h and a maximum d_{eff} of 17 pm/V. The discrepancy can be explained by experimental error and the possibility of weak idler resonance in the crystal.

As shown in Fig. 1, the numerical analysis (which ignores thermal effects) predicts more clamping of the transmitted pump than was observed. Absorption in the periodically poled lithium niobate leads to thermal lensing that affects the coupling among pump, signal, and idler. Thermal effects are indicated by hysteresis in the above-threshold pump power. The inset in Fig. 1 is a plot of the theoretical steady-state pump field as it travels through the periodically poled lithium niobate crystal for three input powers. For increasing input powers the pump field profile curves more owing to growth of the signal field. The pump field at the input must correspondingly increase to provide enough gain for the circulating signal field. As a result, theoretical clamping is not perfect and slopes slightly, as shown in Fig. 1.

The amplitude noise suppression produced by the OPO from dc to 20 kHz is shown in Fig. 2. A constant photocurrent of 4 mA was maintained by an attenuator in front of the detector. For accurate noise measurements we found it necessary to increase the amplitude noise that was present on our input beam by deactivating noise-suppression electronics designed to reduce the laser's relaxation oscillation at 770 kHz. Additional amplification of the detector signal was required so that measurements were not limited by the spectrum analyzer noise.

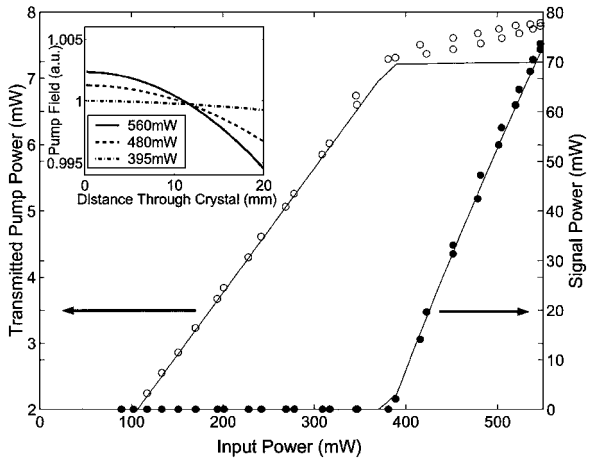

Fig. 1. Steady-state pump and signal OPO output. The experimental results are shown as circles (open, pump; filled, signal), and the theoretical results are shown as lines. The inset shows the theoretical pump field along the periodically poled lithium niobate crystal for three input powers. As input power increases, the field rises at the input so that constant gain is maintained for the signal field, and clamping of the pump output is not perfect.

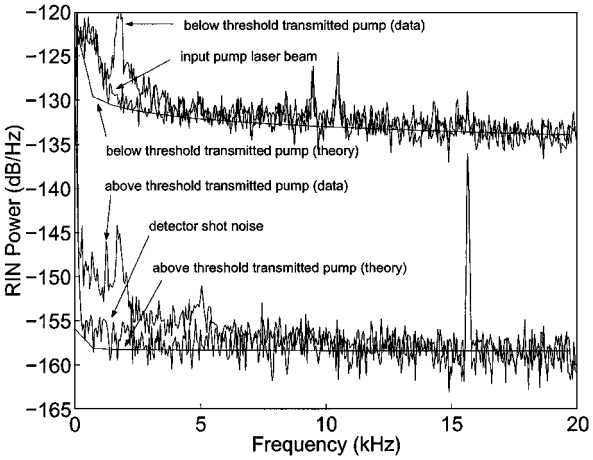

Fig. 2. Relative intensity noise (RIN) power spectra of the transmitted pump, below and above OPO threshold (360- and 380-mW incident pump power, respectively). Theory and measurement show 25 dB of noise suppression above threshold and overlap the detector shot-noise spectrum at frequencies above 7 kHz. All curves were obtained with a photocurrent of 4 mA.

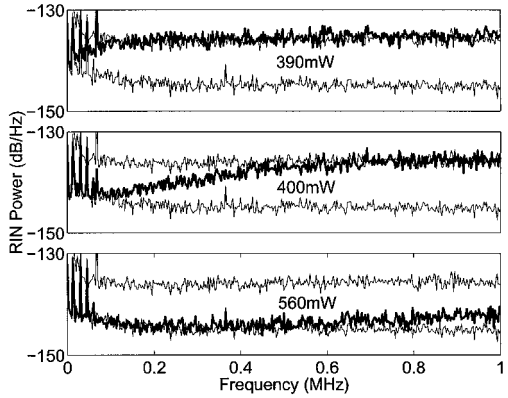

Fig. 3. Relative intensity noise (RIN) suppression up to 1 MHz. The extent of noise suppression depends on the input power (390, 400, and 560 mW shown here). In all plots the top curve shows the input pump, the darker middle curve shows the transmitted pump, and the bottom curve shows the spectrum analyzer noise. Because of reduced input laser noise, we are able to observe only 10 dB of noise suppression before being limited by the spectrum analyzer noise.

Below threshold, the transmitted pump has the same noise spectrum as the input laser, except for a peak near 2 kHz, which we believe to be due to active (piezo) elements in the OPO cavity used for alignment purposes but left unused (shorted) during this experiment. In this regime of operation the OPO acts as an attenuator of the input, and the noise spectrum is unchanged (at frequencies below 1/cavity lifetime $\approx$ 50 MHz). Above threshold, the noise spectrum of the pump beam is reduced by 25 dB to the shot-noise level, over almost the entire frequency range of our measurement. Shot noise was determined with 4 mA of photocurrent, produced by illumination of our detector with incoherent light. The peak at 15.7 kHz, visible in all traces, is from pick-up in the power supply, which disappears if a battery is used. The theoretical trace, which predicts 25 dB of noise reduction, includes shot noise. Both theory and experiment suggest more noise suppression than we are currently able to measure at 7 kHz and above.

Noise suppression at higher frequencies, shown in Fig. 3, depends on the input power (390, 400, and 560 mW are shown here). In all plots the top trace is input noise, the darker middle trace is noise on the transmitted pump beam, and the bottom trace is spectrum analyzer noise. Here, we turned on the laser's noise-suppression electronics to avoid the relaxation-oscillation peak at 770 kHz; these electronics reduce noise from dc to 1 MHz. We were not able to amplify the signal before sending it to the spectrum analyzer, given the bandwidth limitations of our amplifier. Therefore the bottom trace is not detector shot noise but the noise floor of our spectrum analyzer. The input noise is only 10 dB above the spectrum analyzer noise, and 10 dB is the maximum suppression we can measure.

The dependence of noise suppression on input power shown at these higher frequencies is due to the temporal response of the OPO. Just above threshold, a small increase in the input power initially increases the circulating pump field. The signal field, on undergoing this larger gain, will grow, but its rate of growth (in power per unit time) is limited by its initial magnitude. As it started small, the signal field will grow slowly and deplete the resonant pump field slowly. Far above threshold, however, the signal field can change more rapidly, given its initially larger magnitude, and both circulating fields reach steady state more quickly. This can be seen in the numerical analysis, in which just above threshold more iterations are required for the steady state to be reached than are required well above threshold.

In conclusion, we have demonstrated 25 dB of noise suppression from dc to 20 kHz in the transmitted pump of a pump-and-signal-resonant OPO operated above threshold. Additionally, we have demonstrated significant noise suppression up to 1 MHz when the OPO is operated at 130% of threshold power. This noise suppression is explained physically and predicted by numerical analysis. Detection of the full amount of noise suppression is limited by our experiment, and future work will focus on determining the true extent of suppression that is possible with this device and when the useful noise-suppressed pump power is increased.

We thank C. Harb for his design and fabrication of the photoreceiver. This material is based on work supported in whole or in part by National Science Foundation grants NSF PHY-9900793 and NSF PHY-9210038. M. J. Lawrence's e-mail address is matlaw@leland.stanford.edu.

References

1. A. E. Siegman, Appl. Opt. **1,** 739 (1962).
2. J. A. Giordmaine and R. C. Miller, Phys. Rev. Lett. **14,** 973 (1965).
3. T. J. Kane and R. L. Byer, Opt. Lett. **10,** 65 (1985).
4. S. T. Yang, R. C. Eckardt, and R. L. Byer, Opt. Lett. **18,** 971 (1993).
5. W. R. Bosenberg, A. Drobshoff, J. I. Alexander, L. E. Myers, and R. L. Byer, Opt. Lett. **21,** 713 (1996).
6. S. Schiller, K. Schneider, and J. Mlynek, J. Opt. Soc. Am. B **16,** 1512 (1999).
7. M. Arbore and T. McHugh, in *Digest of Conference on Lasers and Electro-Optics* (Optical Society of America, Washington, D.C., 2000), paper CTHQ1.
8. A. Yariv and W. H. Louisell, IEEE J. Quantum Electron. **QE-2,** 418 (1966).
9. J. E. Bjorkholm, Appl. Phys. Lett. **13,** 53 (1968).
10. R. A. Baumgartner and R. L. Byer, IEEE J. Quantum Electron. **QE-15,** 432 (1979).
11. G. D. Boyd and D. A. Kleinman, J. Appl. Phys. **39,** 3597 (1968).
12. L. E. Myers, R. C. Eckardt, M. M. Fejer, R. L. Byer, W. R. Bosenberg, and J. W. Peirce, J. Opt. Soc. Am. B **12,** 2102 (1995).
13. R. W. P. Drever, J. L. Hall, F. V. Kowalski, J. Hough, G. M. Ford, A. J. Munley, and H. Ward, Appl. Phys. B **31,** 97 (1983).
14. S. Guha, F.-J. Wu, and J. Falk, IEEE J. Quantum Electron. **QE-18,** 907 (1982).